九州大学学術情報リポジトリ
Kyushu University Institutional Repository

Determination of Barbiturates by Femtosecond Ionization Mass Spectrometry

Siddihalu, Lakshitha Madunil
Faculty of Design, Kyushu University

Imasaka, Totaro
Kyushu University

Imasaka, Tomoko
Faculty of Design, Kyushu University

https://hdl.handle.net/2324/7153247

出版情報：Analytical chemistry. 92 (42), pp.14691-14698, 2022-10-13. American Chemical Society
バージョン：
権利関係：

KYUSHU UNIVERSITY

Determination of Barbiturates by Femtosecond Ionization Mass Spectrometry

Siddihalu Lakshitha Madunil,[♯] Totaro Imasaka,[†,‡] and Tomoko Imasaka[♯*]

[♯]Faculty of Design, Kyushu University, 4-9-1, Shiobaru, Minami-ku, Fukuoka 815-8540: 744 Motooka, Nishi-ku, Fukuoka 819-0395, Japan
[†]Kyushu University,744 Motooka, Nishi-ku, Fukuoka 819-0395, Japan
[‡]Hikari Giken, Co., 2-10-30, Sakurazaka, Chuou-ku, Fukuoka 810-0024, Japan

ABSTRACT: Barbiturates are highly susceptible to dissociating in mass spectrometry (MS) because of their long side chains combined with a non-aromatic ring consisting of several carbonyl and amine groups. As a result, they exhibit extensive α-cleavage and subsequent rearrangement, making the identification of these compounds difficult. Although a library of electron ionization mass spectrometry (EIMS) is available, most barbiturates have very similar fragment patterns. Accordingly, it would be desirable to develop a technique for soft ionization, providing a molecular ion and large fragment ions as well. In this study, a molecular ion was clearly observed, in addition to large fragment ions, for a variety of barbiturates based on multiphoton ionization mass spectrometry (MPIMS) using a tunable ultraviolet femtosecond laser as the ionization source (fs-LIMS). This favorable result was achieved when the optimal laser wavelength for minimizing the excess energy remaining in the ionic state was used. An examination of the photo fragmentation pathways suggested that a H atom in the side chain was abstracted by an oxygen atom in the carbonyl group in the ring structure thus initiating fragmentation and subsequent rearrangement. Barbiturates that are substituted with alkyl groups (amobarbital and pentobarbital) had narrower spectral regions for optimal ionization than the other barbiturates with alkyl and alkenyl groups (butalbital and secobarbital) and more with alkyl and phenyl groups (phenobarbital). All of the barbiturates studied provided unique mass spectral patterns in fs-LIMS, which was useful for the reliable identification of these compounds in practical trace analysis.

■ INTRODUCTION

Barbiturates are categorized as central nervous system depressants. They have a long history of use as sedatives, hypnotics, anticonvulsant/antiepileptic agents, and as anesthetics as well. Phenobarbital was introduced in 1912 as the first successful psychiatric medication. It is also used to treat gastrointestinal and functional issues associated with asthma.[1] Barbiturates are the earliest and most frequently used sedatives and hypnotics, and they remain popular drugs of abuse among the general public. The therapeutic dose is very close to the fatal dose, and a risk of overdosing is always present when barbiturates are being used. Although barbiturates have adverse synergistic effects, it is difficult to replace them with other drugs as therapeutic drugs and 12 barbiturates continue to be used to treat patients. They are classified as a group of substances with a high potential for abuse and dependency, and deaths have been reported as a result of suppressing respiration when administered in excessive doses. They are frequently employed to commit suicide, homicide, and poisoning by overdose.[2] The analysis of barbiturates in toxicology laboratories is required, because they are still abused and are found in forensic cases.[3]

Barbiturates are analyzed by gas chromatography/nitrogen-phosphorus selective detection/flame ionization detection, gas chromatography/mass spectrometry (GC-MS), liquid chromatography/spectrophotometry, liquid chromatography/mass spectrometry (LC-MS), capillary electrophoresis/multi-wavelength spectrophotometry, and immunoassays.[4-8] Numerous techniques have been employed to measure barbiturates in biological samples. Among them, the most frequently used techniques are GC-MS/MS and LC-MS/MS.[9,10] However, these techniques have a number of disadvantages. For example, the electron ionization (EI) that is currently used in GC-MS and GC-MS/MS results in hard ionization and provides a mass spectrum that consists of dominant fragment ions. It should also be noted that barbiturates easily dissociate with numerous fragment ions being produced because of their long side chains combined with a non-aromatic ring containing several carbonyl and amine groups. In addition, the fragment ions easily undergo rearrangement to produce numerous fragment ions that are very different from a portion of the original structure. Although a library of electron ionization mass spectra (EIMS) is available, most barbiturates have very similar fragment patterns. Accordingly, it would be desirable to develop a technique for soft ionization that provides a molecular ion along with large fragment ions that would permit analogues with very similar chemical structures to be differentiated. On the other hand, electrospray ionization (ESI) currently used in LC-MS and LC-MS/MS is available for soft ionization and provides singly and multiply charged molecular ions with no or less fragment ions, thus making fingerprinting difficult. In addition, resolution in the case of LC is poor and is not suitable for the analysis of a sample that contains a complex matrix. For these reasons, the analytical result is sometimes matrix-dependent as well as component-dependent. A hyphenated MS/MS approach would be useful because of its superior selectivity, in which only the fragment ions produced from a molecular ion or a specified large fragment ion by collision with an inert gas can be measured. However, it is difficult to apply this methodology to a comprehensive analysis of unknown sample mixtures, and the analyte to be measured needs to be determined prior to the analysis.

Photoionization is one of the techniques that have been developed for soft ionization.[11,12] In fact, a molecular ion has been observed in most cases when this

technique is used.[13-15] There are two major approaches to this technique. One is multiphoton ionization (MPI) based on a multiple step transition to exceed the ionization energy. The other is field ionization (FI) based on the tunneling of an electron by a ponderomotive force to exceed the potential barrier by an electric field induced by an intense optical pulse. A Keldysh parameter ($\gamma = (I_p/2U_p)^{1/2} = (E_i/1.87\times10^{-13}I\lambda^2)^{1/2}$) can be used to differentiate the mechanisms of MPI and FI, in which I_p is the potential energy, U_p is the ponderomotive energy, E_i is the zero-field ionization potential expressed in eV, I is the laser intensity in W/cm^2, λ is the laser wavelength in a unit of μm, and the kinetic energy can be calculated by $K = 3.17 \times U_p$.[16,17] When $\gamma > 1$, MPI is a primary ionization process, which is significant when the laser intensity is less than 10^{14} W/cm^2 and the total energy available with several photons exceeds I_p. In contrast, FI is dominant when $\gamma < 1$, and is a major process when a high-peak-power laser emitting at longer wavelengths is tightly focused onto the analyte. Since the sum of the total photon energy and the ponderomotive energy can be used for ionization, both of these ionization processes occur at the boundary of MPI and FI ($\gamma \cong 1$).

Nanosecond and femtosecond lasers are currently used as the ionization sources. A tunable nanosecond laser with a narrow spectral bandwidth is useful for resonance-enhanced multiphoton ionization (REMPI), since selective ionization can be achieved by adjusting the laser wavelength to one of the absorption bands of the analyte. In resonance-enhanced two-photon ionization (RE2PI), one photon is used for the excitation of a molecule to the singlet excited state and a subsequent photon is then used for ionization. However, it is difficult to control the excess energy remaining in the ionic state in one-color RE2PI, when the excitation energy is much larger than half of the ionization energy. A nanosecond laser has been successfully applied for the analysis of an aromatic molecule with an excitation energy that is slightly higher than half of the ionization energy. It should also be noted that an aromatic molecule that is substituted with many halogen atoms or a nitro group has a picosecond/femtosecond lifetime for the singlet excited state. In this case, it would be desirable to ionize the molecule before relaxation to the other electronic state. A femtosecond laser has been employed to solve this problem, since it permits efficient RE2PI even for organohalogen and nitro aromatic hydrocarbons.[13,18] In addition, the femtosecond laser can be utilized for nonresonant 2PI (NR2PI) of organic compounds with no absorption band even in the ultraviolet (UV) region. In this case, the laser wavelength can be adjusted at the half of the ionization energy for 2PI, thus reducing the excess energy to zero. Based on this technique, molecular ions derived from organochlorine pesticides, 4-methylcyclohexanols, amine-related psychoactive substances, and even isotopes of small molecules such as N_2 have been observed.[13,19-21] Although the efficiency of NR2PI is generally lower than that of RE2PI, it approaches a level comparable to RE2PI when a laser pulse width of less than 100 fs is used.[22] It is also noteworthy that photoionization dynamics and ionization efficiencies have been studied using femtosecond lasers.[23-25]

In this study, we examined the optimal laser wavelength required for observing molecular and large fragment ions in RE2PI/NR2PI for several barbiturates with side chains consisting of alkyl, alkenyl, and phenyl groups. The observed data were compared with those measured by FIMS using a near-infrared (NIR) femtosecond laser as the ionization source. For all of the compounds studied here, a mass spectrum measured by RE2PI/NR2PI consisted of a molecular ion, in addition to large fragment

ions. When compared with EIMS data, the relative signal intensity of the molecular ion against the fragment ion was enhanced significantly. This result was preferential for the identification of barbiturates by mass spectrometry. Photo fragmentation pathways were studied to clarify the complex dissociation and rearrangement processes. This technique based on femtosecond laser ionization mass spectrometry (fs-LIMS) was employed for the trace analysis of barbiturates in human urine. The detection limits obtained using molecular and fragment ions were compared with those obtained by other techniques such as GC-EIMS/MS and LC-ESIMS/MS.

■ EXPERIMENTAL

Materials. A standard sample mixture containing five barbiturates, each of which was prepared at a concentration of 250 μg/mL in methanol (1 mL), was obtained from Cerilliant (see the chemical structures in Fig. S1 (A) - (E) in the Supporting Information). The acetone, acetonitrile, and ethyl acetate (analytical grade) used in this study were purchased from Wako Pure Chemical Industries. Extraction salts of QuEChERS for AOAC 2007.01 method (6 g $MgSO_4$ and 1.5 g NaOAc) and dispersive-solid phase extraction tubes (Q-sepTM QuEChERS) for AOAC 2007.01 method (150 mg $MgSO_4$ and 50 mg C18) were purchased from Shimadzu GLC.

Sample Preparation. A stock solution containing the above barbiturates was prepared at a concentration of 20 μg/mL for each by diluting the standard solution with methanol. A series of sample solutions was prepared by diluting it with methanol for the calibration of the signal intensity. A human urine sample from S. L. Madunil was fortified with the standard solution, and the final volume was adjusted to 5.0 mL. The analytes in the fortified urine sample (1.5 mL) were extracted using a modified QuEChERS method, in which the filtration process was removed since it is quick and more reliable and requires only an inexpensive disposable tube for extraction.[26] Accordingly, cross contamination can be avoided and a loss of sample by filtration can be minimal.[27] The solvent was evaporated under nitrogen gas flow and the final volume of the sample solution was filled up to 0.5 mL with ethyl acetate for GC-MS analysis.

Apparatus. The barbiturates mixture was separated by GC (6890N, Agilent Technologies) and measured by TOFMS using an instrument that was developed in our laboratory. The separation column was DB-5ms (length 30 m, inner diameter 0.25 mm, film thickness 0.25 μm). The temperature program of the GC oven was as follows: initial temperature of 60 °C held for 2 min, a rate of 20 °C/min to 320 °C, and held for 10 min. The temperatures of the inlet port and the transfer line between GC and MS were adjusted at 250 and 280 °C, respectively. The flow rate of helium used as a carrier gas was 1 mL/min. A 1 μL aliquot of sample solution was injected into the GC system. A fundamental beam of a Ti/sapphire laser (800 nm, 35 fs, 1 kHz, 6 mJ, Solstice Ace, Spectra-Physics) was used as a pump source for an optical parametric amplifier (OPA, TOPAS Prime, Spectra-Physics). The UV pulses generated at 241, 245, 250, 255, and 260 nm were adjusted at 50 μJ and were used as the ionization sources. The NIR OPA pulse (1300 nm, 600 μJ) was employed for FI to compare the data obtained by MPI. Detail of the computational method is described in the Supporting Information (see the section of Experimental).

■ RESULTS AND DISCUSSION

Ionization Process. The Keldysh parameters calculated under the experimental conditions used in this study are 0.86 - 0.88 and 2.54 - 2.72 for the NIR and UV pulses used in this study, respectively (see the individual values in Table S1 in the Supporting Information). Consequently, 2PI ($\gamma > 1$) was dominant in the UV ionization that occurred at 245 - 255 nm, which was in contrast to FI ($\gamma < 1$) in the NIR ionization at 1300 nm. The spectral properties of barbiturates such as the excitation energy (*EE*) and the ionization energy (*IE*) calculated by density functional theory (DFT) are shown in Figs. S2-S6 (absorption spectra calculated for neutral and ionic species), and the results are summarized in Table 1. Accordingly, barbiturates have a small absorption band in

Table 1 Calculated spectral properties and observed data for the barbiturates

Compound	Mw [a]	*EE* [b] eV (nm)	*IE* [c] eV (nm)	IE_{opt} [d] eV (nm)	ΔE [e] eV	M^+/F^+ [f]	EF[g]
Butalbital	224	5.02 (247)	9.64 (257/2)	10.20 (243/2)	0.56	0.88	-
Amobarbital	226	5.02 (247)	9.91 (250/2)	10.16 (244/2)	0.25	1.9	-
Pentobarbital	226	4.95 (251)	9.85 (252/2)	10.12 (245/2)	0.27	0.60	-
Secobarbital	238	4.95 (250)	9.52 (260/2)	10.08 (246/2)	0.56	0.70	40
Phenobarbital	232	4.94 (251)	9.34 (265/2)	9.72 (255/2)	0.38	21	200

a) molecular weight; b) excitation energy calculated by DFT; c) ionization energy calculated by DFT; d) optimal photon energy for observing a molecular ion (see the data shown in Fig. 2); e) excess energy calculated by d) – c); f) ratio of the signal intensities measured for a molecular ion (M^+) and a fragment ion (F^+) specified in Fig. 2; g) enhancement factor defined as a ratio of the M^+/F^+ values obtained by fs-LIMS and EIMS; -, a molecular ion is not observed in the NIST EIMS database.

the 240-260 nm region, due to a conjugated hetero-ring structure, as shown in Fig. S1. However, the molar absorptivities are rather small (ε = 670 - 1400 mol^{-1} cm^{-1}) (oscillator strengths = 0.0001 - 0.0004), suggesting near-RE2PI or NR2PI processes. It should also be noted that fragmentation can be accelerated when a "molecular ion" absorbs a subsequent photon because of the large excess energy to be used for dissociation. The molar absorptivities of the molecular ion are similar to or slightly smaller (ca. 5×10^2) in the UV (240-250 nm) and NIR (1300 nm) regions, when compared with those of neutral species. Therefore, auto-dissociation from the ionic state appears to be the major fragmentation process, although the possibility of photo dissociation induced by FI and/or the subsequent absorption of an NIR photon due to a large output power of the NIR laser being used cannot be excluded.

Two-dimensional Display. A two-dimensional display was measured at 250 nm by GC combined with time-of-flight mass spectrometry (GC-TOFMS) for a sample mixture containing butalbital, amobarbital, pentobarbital, secobarbital, and phenobarbital to visually compare the mass spectra and the results are shown in Fig. 1.

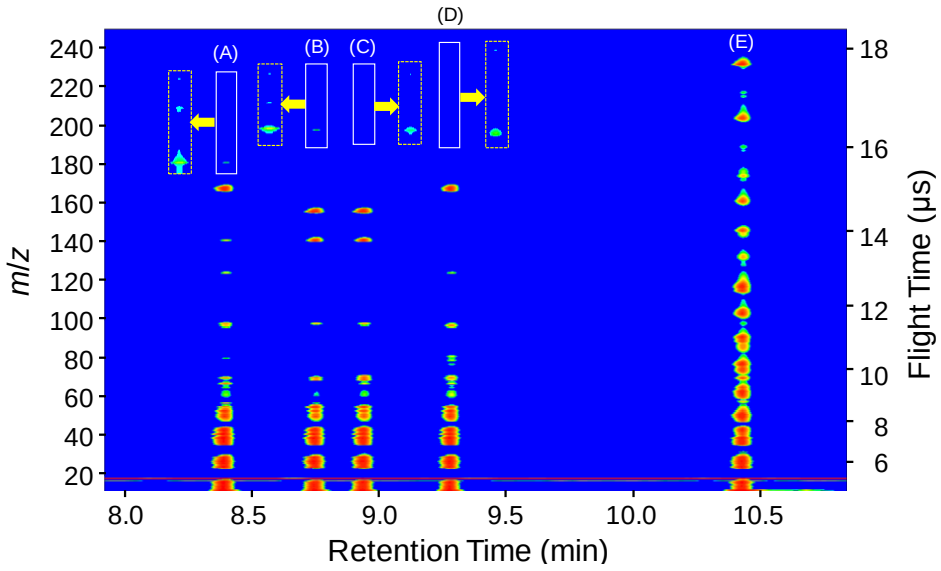

Fig. 1. Two-dimensional display obtained for a sample mixture containing five different barbiturates (20 μg/mL for each) measured at 250 nm. Assignment: (A) butalbital (B) amobarbital (C) pentobarbital (D) secobarbital (E) phenobarbital. The signals in the squares specified by solid lines are 50 times intensified, which are shown in the squares specified by broken lines.

Note that the two-dimensional display measured in the NIR region is shown in Fig. S7 (two-dimensional data observed at 1300 nm). The organic compounds such as barbiturates can be separated by the DB-5MS column, depending on the polarity and the volatility of the analyte. Phenobarbital has an induced dipole and is more polar than the aliphatic four compounds, thus eluting at the end. When considering the molecular weights (volatility), the retention time increases in the order of butalbital, amobarbital, pentobarbital and secobarbital. In general, barbiturates are very prone to dissociation and provide numerous fragment ions at small mass-to-charge ratios (m/z). It should be noted that molecular ions are typically not observed for barbiturates except for secobarbital and phenobarbital in EIMS as reported in the National Institute of Standards and Technology (NIST) database. However, a molecular ion was clearly observed in fs-LIMS for all of the barbiturates that were examined in this study. In contrast, no molecular ion was observed at 1300 nm. This undesirable result can be attributed to the efficient dissociation by FI (or photo dissociation by absorbing an additional NIR photon). These data suggest that the UV 2PI is more preferential for observing a molecular ion.

Wavelength Dependence. Figure 2 shows the ratio of the signal intensities measured for molecular and fragment ions, M^+/F^+, at different wavelengths, indicating that the intensity of the molecular ion can be enhanced significantly when the laser wavelength is optimized in the spectral region of 243-255 nm. This result suggests that barbiturates are very susceptible to undergoing photo dissociation, probably due to the presence of carbonyl and amine groups and the low-frequency vibrational modes arising from flexible bulky groups in the side chain, which would accelerate the dissociation. As reported, the ratio decreases at shorter wavelengths with a gradual increase in excess energy by 2PI and decreases significantly at longer wavelengths with a substantial increase in excess energy by 3PI.[19,20] Note that RE2PI contributes more at shorter wavelengths for barbiturates (see Figs. S2-S6). The optimal ionization energy (IE_{opt}),

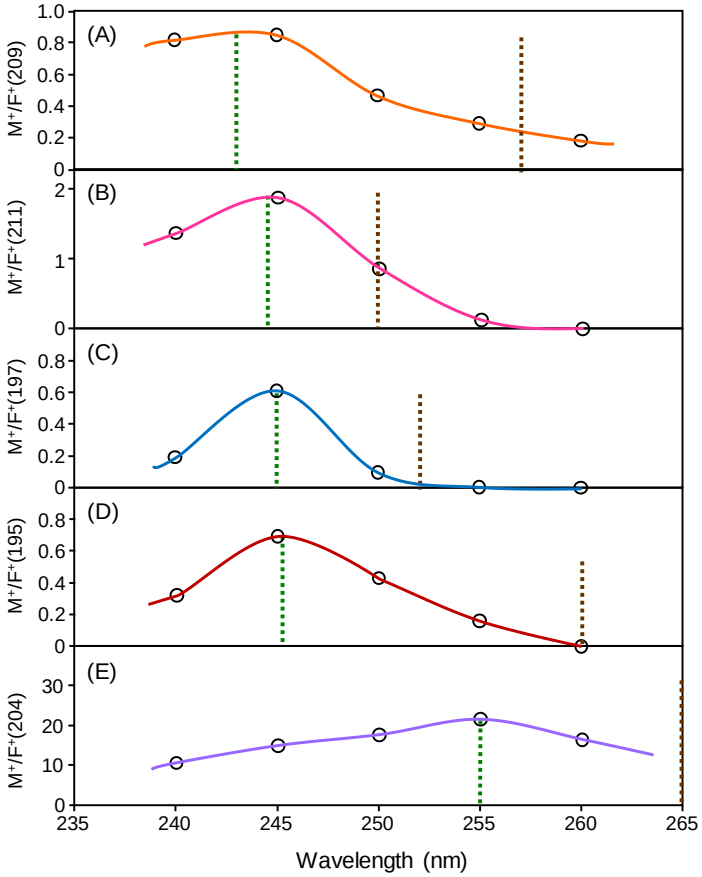

Fig. 2. Dependence of the ratio of the signal intensities observed for molecular and fragment ions on the laser wavelength. The *m*/*z* value of the fragment ion is specified in parenthesis. (A) butalbital (B) amobarbital (C) pentobarbital (D) secobarbital (E) phenobarbital.

defined as the two-photon energy at the signal peak in Fig. 2, and the excess energy (ΔE), defined as the value of $IE_{opt} - IE$, are summarized in Table 1. The excess energy optimal for 2PI was 0.25 - 0.56 eV for barbiturates. These values were similar to those observed for very photo dissociative compounds such as *cis*- and *trans*-4-methylcyclohexanols and psychoactive substances that contain amine groups, which were much smaller than the ca. 3 eV observed for ordinary organic compounds.[19,20,28] It is interesting to note that the M^+/F^+ values observed for amobarbital and pentobarbital, which both contain only alkyl side chains, decreased more rapidly at longer wavelengths than those for butalbital and secobarbital with alkyl and alkenyl side chains. In addition, a molecular ion was observed only when ΔE was adjusted to be minimal for amobarbital (0.25 eV) and pentobarbital (0.27 eV) rather than for butalbital (0.56 eV) and secobarbital (0.56 eV). These findings can be explained by the ionic state being stabilized with delocalized π electrons in the side chain. Moreover, phenobarbital has a flatter wavelength dependence, since the ionic state can be more efficiently stabilized by a phenyl group with a larger number of π electrons. It should also be noted that a molecular ion for a barbiturate molecule has an absorptivity of 300 - 1500 mol^{-1} cm^{-1} at 250 nm, which is comparable to the molar absorptivity of the neutral species. As a result, both processes, namely, auto-dissociation after ionization and photo dissociation after the subsequent absorption of an additional photon can occur in this

study. Since barbiturates contain many groups that can dissociate and readily rearrange, the excess energy should be minimal for observing a molecular ion.

Mass Spectra for Barbiturates. Figure 3 shows mass spectra measured for barbiturates at the optimal wavelengths (see the caption). Extensive fragmentation was observed due to efficient α-cleavage and subsequent McLafferty rearrangement. However, a molecular ion was clearly observed in addition to large fragment ions for all of the barbiturates that were examined in fs-LIMS. In contrast, no molecular ions are observed for barbiturates in the NIST EIMS data, except for secobarbital and phenobarbital.[29-33] Due to the highly flexible structure of barbiturates, the contribution of adiabatic ionization would be negligible. Therefore, a molecular ion produced by vertical ionization from the ground state would have sufficient internal energy and would undergo efficient fragmentation. Accordingly, the excess energy should be minimal for observing a molecular ion. Two alkyl groups are substituted at the α-C position in the hetero ring for amobarbital and pentobarbital. Their fragment patterns are very similar, since they are structural isomers. However, a sharp signal peak was observed at m/z = 211 only for amobarbital, which can be used for differentiating amobarbital and pentobarbital. On the other hand, butalbital and secobarbital both contain an alkenyl side chain and have nearly identical fragment patterns. However, a molecular ion was observed at m/z = 224 and 226 for butalbital and secobarbital, respectively, showing that they can be differentiated in fs-LIMS. For phenobarbital, the

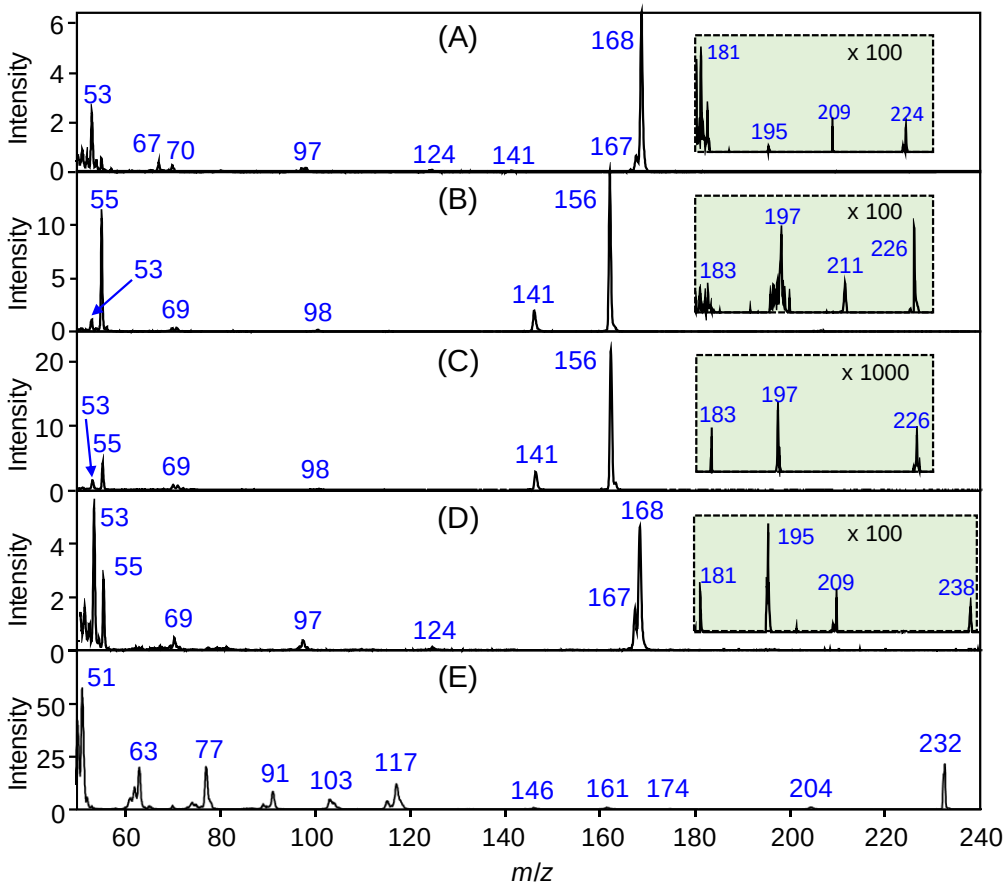

Fig. 3 Mass spectra observed for (A) butalbital (B) amobarbital (C) pentobarbital (D) secobarbital (E) phenobarbital at (A) - (D) 245 nm (E) 255 nm.

mass spectral pattern was completely different from those for the other barbiturates due to the presence of a more stable phenyl group in the side chain.

Photo Fragmentation Pathways: Amobarbital and Pentobarbital. Possible fragmentation pathways for amobarbital are shown in Fig. S8 (four major fragmentation processes (A) - (D) of amobarbital). The abstraction of a H atom in the side chain by an oxygen atom in the carbonyl group initiates the fragmentation, which is followed by the elimination of CH_3, C_2H_5, and C_3H_7 groups from the side chain in the vicinity of the carbonyl group, providing large fragment ions at (A) m/z = 211, (B) m/z = 197, and (C) m/z = 183, respectively, as shown in Figs. S8 (A) – (C). As discussed above, the characteristic peak at m/z = 211 can be used for the identification of this compound. Another pathway involves the dissociation of 3-methyl-1-butene, as shown in Fig. S8 (D). Two major fragment ions were observed at m/z = 156 and 141 in the mass spectrum, since they are stabilized by the delocalization of π electrons in the hetero ring. Further dissociation by the fragmentation of the ring structure provided a smaller fragment ion at m/z = 98.

Possible fragmentation pathways for pentobarbital are shown in Fig. S9 (three major fragmentation processes (A) - (C) of pentobarbital). Similar to amobarbital, the fragmentation involves the elimination of a CH_3 group, with the production of a fragment ion at m/z = 211, as shown in Fig. S9 (A). However, this fragment ion was not observed in the mass spectrum, since it readily produces a fragment ion at m/z = 183 via the dissociation of CO. Note that formation of a CO molecule would be energetically favorable ($\Delta_f H°_{gas}$ = -110.53 kJ/mol),[34] which would accelerate this reaction. This result is in contrast to the case of amobarbital, in which a fragment ion was observed at m/z = 211. A tertiary carbon atom in the middle of the alkyl chain would make this fragment ion more unstable because of the congested chemical structure in the side chain.

Photo Fragmentation Pathways: Butalbital and Secobarbital. Butalbital and secobarbital both have an alkenyl side chain. The only difference is the position of the CH_3 group and the length of the side chain (see Fig. S1). Accordingly, the mass spectral patterns for these 2 compounds were very similar, except for the observation of a molecular ion at m/z = 224 and 238 for butalbital and secobarbital, respectively. As mentioned above, observing a molecular ion is essential for the reliable differentiation of these compounds. In Figs. 3 (A) and (D), two major fragment ions were observed at m/z = 168 and 167 in the mass spectra. Possible fragmentation pathway for butalbital are shown in Fig. S10 (three major fragmentation processes (A) - (C) of butalbital). As shown in Fig. S10 (A), the elimination of a CH_3 group produces a fragment ion at m/z = 209, which further dissociates CO to form a fragment ion at m/z = 181 by breaking the hetero ring structure. As shown in Figs. S10 (B) and (C), the elimination of C_2H_5, C_4H_8, and C_4H_9 groups produces fragment ions at m/z = 195, 168, and 167, respectively. The latter two fragment ions are stabilized by the delocalization of π electrons in the hetero ring, providing large signals in the mass spectrum. As shown in Fig. S10 (C-2), a positive charge on the carbon atom in an aliphatic ether ring is less stabilized than a positive charge on the oxygen atom (see Fig. S10 (C-1)). As a result, the fragment ion at m/z = 167 undergoes further dissociation to produce smaller fragment ions, providing a weaker signal intensity than the signal at m/z = 168.

Possible fragmentation pathways for secobarbital are shown in Fig. S11 (three major fragmentation processes (A) - (C) of secobarbital). The signal peak at m/z = 195 is more intense than that for butalbital as shown in Fig. 3 (D). This is probably due to

stabilization of the fragment ion by the elimination of a larger C_3H_7 group (cf. Figs. S10 (B) and S11 (B)), since the excess energy in the ionic state can be partly lost in the form of internal energy of the C_3H_7 group. In addition, the fragment ion at m/z = 181 formed by α-cleavage and the dissociation of CO was relatively smaller for secobarbital than the fragment ion at m/z = 181 for butalbital, which can be explained by the formation of a more unstable fragment ion consisting of an asymmetric structure of the side chain. In the NIST EIMS database, the signal intensity of the molecular ion for secobarbital is very weak (no signal for butalbital). It should be noted that the ratio of M^+/F^+ was, however, enhanced 40-fold by using fs-LIMS (see Table 1). Accordingly, fs-LIMS can be successfully used for the differentiation of these compounds.

Photo Fragmentation Pathways: Phenobarbital. Possible fragmentation pathways for phenobarbital are shown in Fig. S12 (five major fragmentation processes (A) - (E) of phenobarbital). A molecular ion at m/z = 232 is stabilized by a phenyl group substituted at the α-C position and is observed as one of the major signals in the mass spectrum, which is in contrast to the other barbiturates that contain flexible alkyl/alkenyl side chains. The fragment ion at m/z = 204 is also stabilized by a conjugated phenyl group (see Fig. S12 (A)), which is observed as a base peak in the NIST EIMS database. In fs-LIMS, the excess energy is minimal, and the fragment ion at m/z = 204 is suppressed significantly. In fact, the ratio of M^+/F^+ was enhanced by 200-fold when compared with EIMS (see Table 1). Due to a bulky phenyl group with low-frequency vibrational modes, the energy remaining in the ionic state is efficiently distributed to a hetero ring system, which undergoes dissociation to many fragment ions that are observed at (B) m/z = 161 and 117, (C) m/z = 174, (D) m/z = 103 and subsequently (D-1) m/z = 91 (D-2) m/z = 77, 63, 51, and (E) m/z = 146 (see Fig. S12).

Real Sample. A sample mixture containing five barbiturates was spiked in human urine and was analyzed to demonstrate availability of fs-LIMS for measuring a real sample in a matrix containing interferences. As shown in Fig. 4, the barbiturates studied

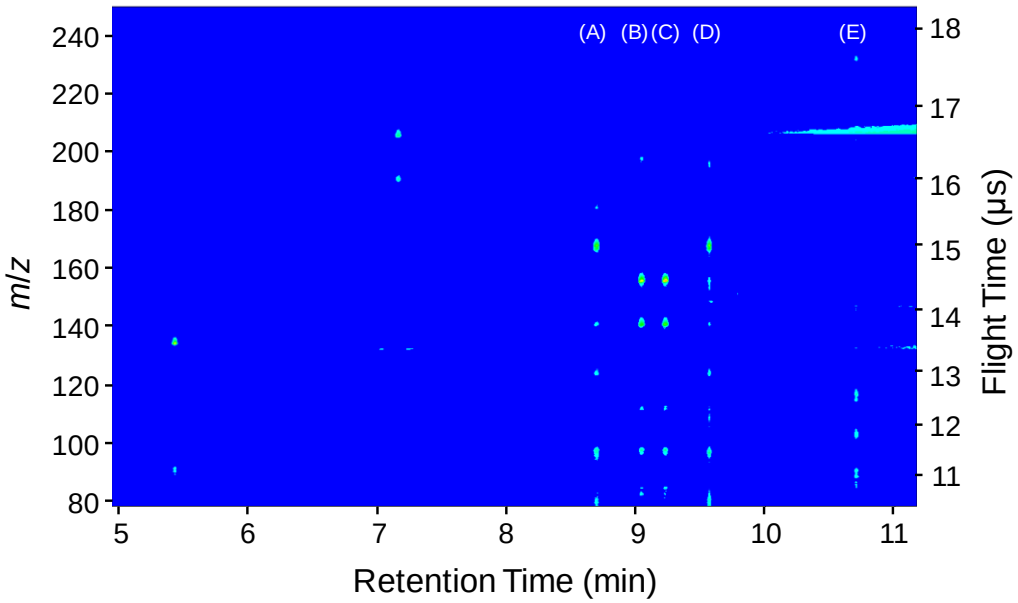

Fig. 4. Two-dimensional display for a urine sample containing barbiturates (2 μg/mL for each) measured at 250 nm, 50 mW. (A) butalbital (B) amobarbital (C) pentobarbital (D) secobarbital (E) phenobarbital.

here were clearly identified on the two-dimensional display of GC-MS. It should also be noted that the background signal arising from interference was supressed significantly by combining fs-LIMS with modified QuEChERS. The limits of detection (LODs) achieved for barbiturates using the signal of a molecular ion (a fragment ion) were 2.9 (4.8) ng/mL for phenobarbital and 110-270 (2.9-4.4) ng/mL for the other barbiturates (see the LODs for individual compounds in Table S2). The low value of LOD achieved using a molecular ion for phenobarbital would be due to near-RE2PI at 250 nm. The analytical curve was linear in the 0-5000 ng/mL range, the correlation coefficient being 0.972 – 0.989 (see the individual data in Table S3). Note that therapeutic, toxic, and fatal concentrations in human blood are reported to be > 1000 ng/mL.[35,36] The technique described herein can be applied to the analysis of clinical and forensic samples.

Comparison. The LODs measured for a urine sample using conventional GC-MS combined with solid-phase extraction and direct immersion solid-phase microextraction are reported to be 10-80 and 10-600 ng/mL, respectively.[5,37] On the other hand, the LODs obtained using LC-MS by the direct injection of a urine sample after simple filtration are reported to be 660-2700 ng/mL.[38] Lower LODs have been achieved using a multiple reaction monitoring technique in MS/MS. The LODs measured for barbiturates in human blood using GC-EIMS/MS and LC-ESIMS/MS are reported to be 0.36-0.78 and 70-320 ng/mL, respectively.[39,40] As mentioned above, these techniques are, however, not applicable for a comprehensive analysis, and the components to be measured need to be known prior to the measurement. In addition, barbiturates provide very similar patterns in the mass spectrum, and the retention index is nearly identical for structural isomers such as amobarbital (1741) and pentobarbital (1767). Thus, identifying these compounds, even when a fused-silica capillary was employed as a column for GC separation, is not a straightforward task.[39] It should be noted that fs-LIMS providing large fragment ions (e.g., observed at m/z = 211 for amobarbital) can be used for the differentiation of even isomers such as amobarbital and pentobarbital. Note that the structural isomers such as ortho-, meta-, and para-fluorotoluene have been differentiated by means of chirped fs-LIMS without using a technique of chromatographic separation.[24] On the other hand, EIMS provides numerous fragment ions and atmospheric-pressure chemical ionization provides no or few fragment ions in the mass spectrum, thus providing limited structural information.[41] It should be noted that many types of barbiturates and their analogues have been developed to date. For example, thiopental (F) can be evaluated by measuring the concentration of pentobarbital (C), a metabolite of thiopental (F) (see Fig. S1 for the chemical structures). On the other hand, phenobarbital (E) is a metabolite of methylphenobarbital (G) and primidone (H).[36] The present technique based on GC-TOFMS is useful for the comprehensive analysis of these compounds in human urine.

Future Studies. Further improvement in LODs could be achieved by pre-concentrating the sample solution due to the low background signal in fs-LIMS as shown in Fig. S13 (two-dimensional display of the blank sample). Note that the sample has been pre-concentrated 5-fold from 200 to 40 μL for a blood sample measured by the aforementioned GC-EIMS/MS.[39] Accordingly, the LODs reported in this study could likely be improved to a level comparable to this method. Another possibility would be the use of the fourth harmonic emission (257 nm) of a highly-repetitive high-average-power femtosecond Yb laser (1030 nm) combined with a time-correlated single ion counting system because of the lower cost and higher sensitivity.[42] The sixth harmonic

emission (250 nm) of a femtosecond Er laser (1500 nm) would be more successful for better spectral matching of the laser wavelength with the optimal values (243-255 nm) for observing a molecular ion.

■ CONCLUSION

A sample mixture of barbiturates was separated by GC and measured by fs-LIMS to suppress the fragmentation. The optimal laser wavelength for observing a molecular ion was in the 243-255 nm range, which corresponds to near-RE2PI for phenobarbital and NR2PI for the other barbiturates. Due to the photo dissociative nature of barbiturates, the excess energy in the ionic state should be minimal (< 0.5 eV), because of the presence of a hetero ring consisting of several nitrogen and oxygen atoms. This approach based on 2PI using a UV femtosecond laser was superior to FI using an NIR laser and EI as well for observing a molecular ion. Photo fragmentation pathways were also investigated in this study, which is initiated by the abstraction of a H atom from the side chain followed by fragmentation and subsequent rearrangement. By using fs-LIMS, the ratio of M^+/F^+ was enhanced significantly (40-200 fold) in comparison with EIMS. The stability of the molecular ion depends on the substituted group, and the phenyl group was the most effective for suppressing the fragmentation by stabilizing the π electrons in the hetero-ring. A two-dimensional display of GC-TOFMS was measured for the trace analysis of barbiturates in human urine. Due to superior selectively achieved by fs-LIMS, the background signal was suppressed, even though a simple pre-treatment procedure was used prior to the GC-MS analysis. The LODs for the barbiturates were measured using the molecular ions and were found to be sufficiently low to permit these compounds to be detected at therapeutic, toxic, and fatal concentrations. The LODs were further improved by using the fragment ions for barbiturates with no phenyl group. This approach, which is based on tunable UV fs-LIMS, can be used as a universal tool for the measurement of organic compounds, since the molecular ion can be enhanced by adjusting the photon energy to be slightly above half of the ionization energy. As a result, this technique can be successfully used for observing a molecular ion even for a molecule that dissociates easily with the formation of fragment ions with a minimal excess energy in various application fields including environmental and forensic sciences.

■ ASSOCIATED CONTENT

Supporting Information

The Supporting Information is available free of charge at
https://pubs/acs.org/doi/

■ AUTHOR INFORMATION

Corresponding Author

Tomoko Imasaka - *Faculty of Design, Kyushu University, 4-9-1, Shiobaru, Minami-ku, Fukuoka 815-8540: 744 Motooka, Nishi-ku, Fukuoka 819-0395, Japan*
ORCID: 0000-0002-2131-4995; Email: imasaka@design.kyushu-u.ac.jp

Authors

Siddihalu Lakshitha Madunil - *Faculty of Design, Kyushu University, 4-9-1, Shiobaru, Minami-ku, Fukuoka 815-8540: 744 Motooka, Nishi-ku, Fukuoka 819-0395, Japan*
ORCID: 0000-0002-8454-9556; Email: madunils@yahoo.com

Totaro Imasaka - *Kyushu University, 744 Motooka, Nishi-ku, Fukuoka 819-0395, Japan*
Hikari Giken, Co., 2-10-30, Sakurazaka, Chuou-ku, Fukuoka 810-0024, Japan
ORCID: 0000-0003-4152-3257; Email: TotaroImasaka@gmail.com

Author Contributions

Siddihalu L. Madunil: Performed the experimental work and wrote the original draft.
Totaro Imasaka: Supervision and revision of the draft.
Tomoko Imasaka: Funding acquisition, supervision, and computational calculations.

Notes

The authors declare no competing financial interest.

■ ACKNOWLEDGMENTS

This research was supported by a Grant-in-Aid for Scientific Research from the Japan Society for the Promotion of Science [JSPS KAKENHI Grant Numbers 20H02399] and by the Heiwa Nakajima Foundation and the AMADA Foundation. Quantum chemical calculations were mainly carried out using the computer facilities at the Research Institute for Information Technology, Kyushu University. L. M. wishes to acknowledge the Mitsubishi Corporation International Scholarship for financial support to study in Japan.

■ REFERENCES

(1) López-Muñoz, F.; Ucha-Udabe, R.; Alamo, C. The history of barbiturates a century after their clinical introduction. *Neuropsychiatric Disease and Treatment* **2005**, 1, 329-343.

(2) Russell, J. M.; Newman, S. C.; Bland, R. C. Drug abuse and dependence, *Acta Psychiatr. Scand.* **1994**, 89, 54-62.

(3) Nishimura, M.; Bhatia, H.; Ma, J.; Dickson, S. D.; Alshawabkeh, L.; Adler, E.; Maisel, A.; Criqui, M. H.; Greenberg, B.; Thomas, I. C. The impact of substance abuse on heart failure hospitalizations. *Am. J. Med.* **2020**, 133, 207-213.

(4) Kinberger, B.; Holmén, A.; Wahrgren, P. Determination of barbiturates and some neutral drugs in serum using quartz glass capillary gas chromatography. *J. Chromatogr. B Biomed. Appl.* **1981**, 224, 449-455.

(5) Iwai, M.; Hattori, H.; Arinobu, T.; Ishii, A.; Kumazawa, T.; Noguchi, H.; Noguchi, H.; Suzuki, O.; Seno, H. Simultaneous determination of barbiturates in human biological fluids by direct immersion solid-phase microextraction and gas chromatography–mass spectrometry. *J. Chromatogr. B* **2004**, 806, 65-73.

(6) García-Borregón, P. F.; Lores, M.; Cela, R. Analysis of barbiturates by micro-high-performance liquid chromatography with post-column photochemical derivatization. *J. Chromatogr. A* **2000**, 870, 39-44.

(7) Thormann, W.; Meier, P.; Marcolli, C.; Binder, F. Analysis of barbiturates in human serum and urine by high-performance capillary electrophoresis-micellar electrokinetic capillary chromatography with on-column multi-wavelength detection. *J. Chromatogr. A* **1991**, 545, 445-460.

(8) Schwenzer, K. S.; Pearlman, R.; Tsilimidos, M.; Salamone, S. J.; Cannon, R. C.; Wong, S. H. Y.; Gock, S. B.; Jentzen, J. J. New fluorescence polarization immunoassays for analysis of barbiturates and benzodiazepines in serum and urine: performance characteristics. *J. Anal. Toxicol.* **2000**, 24, 726-732.

(9) Zhao, H.; Wang, L.; Qiu, Y.; Zhou, Z.; Zhong, W.; Li, X. Multiwalled carbon nanotubes as a solid-phase extraction adsorbent for the determination of three barbiturates in pork by ion trap gas chromatography-tandem mass spectrometry (GC/MS/MS) following microwave assisted derivatization. *Anal. Chim. Acta* **2007**, 586, 399-406.

(10) Feng, J.; Wang, L.; Dai, I.; Harmon, T.; Bernert, J. T. Simultaneous determination of multiple drugs of abuse and relevant metabolites in urine by LC-MS-MS. *J. Anal. Toxicol.* **2007**, 31, 359-368.

(11) Boesl, U.; Zimmermann, R.; Weickhardt, C.; Lenoir, D.; Schramm, D. W.; Kettrup, A.; Schlag, E. W. Resonance-enhanced multi-photon ionization: a species-selective ion source for analytical time-of-flight mass spectroscopy. *Chemosphere* **1994**, 29, 1429-1440.

(12) Mitschke, S.; Welthagen, W.; Zimmermann, R. Comprehensive gas chromatography-time-of-flight mass spectrometry using soft and selective photoionization techniques. *Anal. Chem.* **2006**, 78, 6364-6375.

(13) Madunil, S. L.; Imasaka, T.; Imasaka, T. Resonant and nonresonant femtosecond ionization mass spectrometry of organochlorine pesticides. *Analyst* **2020**, 145, 777-783.

(14) Giri, A.; Coutriade, M.; Racaud, A.; Okuda, K.; Dane, J.; Cody, R. B.; Focant, J-F. Molecular characterization of volatiles and petrochemical base oils by photo-ionization GC×GC-TOF-MS. *Anal. Chem.* **2017**, 89, 5395-5403.
(15) DeWitt, M. J.; Peters, D. W.; Levis, R. J. Photoionization/dissociation of alkyl substituted benzene molecules using intense near-infrared radiation. *Chem. Phys.* **1997**, 218, 211-223.
(16) Keldysh, L. V. Ionization in the field of a strong electromagnetic wave. *Sov. Phys. JETP* **1965**, 20, 1307-1314.
(17) Agostini, P.; Fabre, F.; Mainfray, G.; Petite, G. N.; Rahman, K. Free-free transitions following six-photon ionization of xenon atoms. *Phys. Rev. Lett.* **1979**, 42, 1127-1130.
(18) Lemire, G. W.; Simeonsson, J. B.; Sausa, R. C. Monitoring of vapor-phase nitro compounds using 226-nm radiation: fragmentation with subsequent NO resonance-enhanced multiphoton ionization detection. *Anal. Chem.* **1993**, 85, 529-533.
(19) Madunil, S. L.; Imasaka, T.; Imasaka, T. Suppression of fragmentation in mass spectrometry. *Anal. Chem.* **2020**, 92, 16016-16023.
(20) Madunil, S. L.; Imasaka, T.; Imasaka, T. Comprehensive analysis of analogues of amine-related psychoactive substances using femtosecond laser ionization mass spectrometry. *J. Am. Soc. Mass Spectrom.* **2022**, 33, 90-99.
(21) Akagi, H.; Kasajima, T.; Kumada, T.; Itakura, R.; Yokoyama, A.; Hasegawa, H.; Ohshima, Y. Isotope-selective ionization utilizing molecular alignment and nonresonant multiphoton ionization. *Appl. Phys. B* **2012**, 109, 75-80.
(22) Kouno, H.; Imasaka, T. The efficiencies of resonant and nonresonant multiphoton ionization in the femtosecond region. *Analyst* **2016**, 141, 5274-5280.
(23) Zhu, X.; Lozovoy, V. V.; Shah, J. D.; Dantus, M. Photodissociation dynamics of acetophenone and its derivatives with intense nonresonant femtosecond pulses. *J. Phys. Chem. A* **2011**, 115, 1305-1312.
(24) Schafer, V.; Weitzel, K.-M. Qualitative and quantitative distinction of ortho-, meta-, and para-fluorotoluene by means of chirped femtosecond laser ionization. *Anal. Chem.* **2020**, 92, 5492-5499.
(25) Tibbetts, K. M., Coherent vibrational and dissociation dynamics of polyatomic radical cations. *Chem. Eur. J.* **2019,** 25, 8431-8439.
(26) Kusano, M; Sakamoto, Y; Natori, Y; Miyagawa, H; Tsuchihashi, H; Ishii, A; Zaitsu, K. Development of "Quick-DB forensic": A total workflow from QuEChERS-dSPE method to GC–MS/MS quantification of forensically relevant drugs and pesticides in whole blood. *Forensic Sci. Int.* **2019**, *300*, 125-135.
(27) Carlson, M.; Thompson, R. D. Analyte loss due to membrane filter adsorption as determined by high-performance liquid chromatography. *J. Chromatogr. Sci.* **2000**, *38*, 77-83.
(28) Shibuta, S.; Imasaka, T.; Imasaka, T. Determination of fragrance allergens by ultraviolet femtosecond laser ionization mass spectrometry. *Anal. Chem.* **2016**, 88, 10693-10700.
(29) National Institute of Standards and Technology, https://webbook.nist.gov/cgi/cbook.cgi?ID=C77269&Units=SI&Mask=200#Mass-Spec (accessed 2022-04-08).

(30) National Institute of Standards and Technology, https://webbook.nist.gov/cgi/cbook.cgi?ID=C57432&Units=SI&Mask=200#Mass-Spec (accessed 2022-04-08).
(31) National Institute of Standards and Technology, https://webbook.nist.gov/cgi/cbook.cgi?ID=C76744&Units=SI&Mask=200#Mass-Spec (accessed 2022-04-08).
(32) National Institute of Standards and Technology, https://webbook.nist.gov/cgi/cbook.cgi?ID=C76733&Units=SI&Mask=200#Mass-Spec (accessed 2022-04-08).
(33) National Institute of Standards and Technology, https://webbook.nist.gov/cgi/cbook.cgi?ID=C50066&Units=SI&Mask=200#Mass-Spec (accessed 2022-04-08).
(34) Cox, J. D.; Wagman, D. D.; Medvedev, V. A. CODATA key values for thermodynamics. Hemisphere Publishing Corp., New York, 1989.
(35) Winek, C. L.; Wahba, W. W.; Winek, C. L. Jr.; Balzer, T. W. Drug and chemical blood-level data 2001. *Forensic Sci. Int.* **2001**, 122, 107-123.
(36) Moffat, A. C.; Osselton, M. D.; Widdop, B.; Watts, J. Monographs. In Clarke's analysis of drugs and poisons in pharmaceuticals, body fluids and postmortem material, 4th ed.; Pharmaceutical Press: London, 2011; pp 890-2050.
(37) Chou, H-Y.; Chang, W-T.; Wang, C-T.; Liang, Y-Hung. Optimal parameters for the GC/MS quantitation of barbiturates in urine at lower concentration levels. *Forensic Sci.* **2012**, 11, 25-32.
(38) Martín-Biosca, Y.; Sagrado, S.; Villaneuva-Camañas, R. M.; Medina-Hernández, M. J. Determination of barbiturates in urine by micellar liquid chromatography and direct injection of sample. *J. Pharm. Biomed.* **1999**, 21, 331-338.
(39) Kusano, M; Sakamoto, Y; Natori, Y; Miyagawa, H; Tsuchihashi, H; Ishii, A; Zaitsu, K. Development of "Quick-DB forensic": A total workflow from QuEChERS-dSPE method to GC–MS/MS quantification of forensically relevant drugs and pesticides in whole blood. *Forensic Sci. Int.* **2019**, 300, 125-135.
(40) Sørensen, L. K. Determination of acidic and neutral therapeutic drugs in human blood by liquid chromatography-electrospray tandem mass spectrometry. *Forensic Sci. Int.* **2011**, 206, 119-126.
(41) Jones, J. J.; Kidwell, H.; Games, D. E. Application of atmospheric pressure chemical ionization mass spectrometry in the analysis of barbiturates by high speed analytical countercurrent chromatography. *Rapid Commun. Mass Spectrom.* **2003**, 17, 1565-1572.
(42) Yoshinaga, K.; Hao, N. V.; Imasaka, T.; Imasaka, T. Miniature time-of-flight mass analyzer for use in combination with a compact highly-repetitive femtosecond laser ionization source. *Anal. Chim. Acta* **2022**, 1203, 339673.

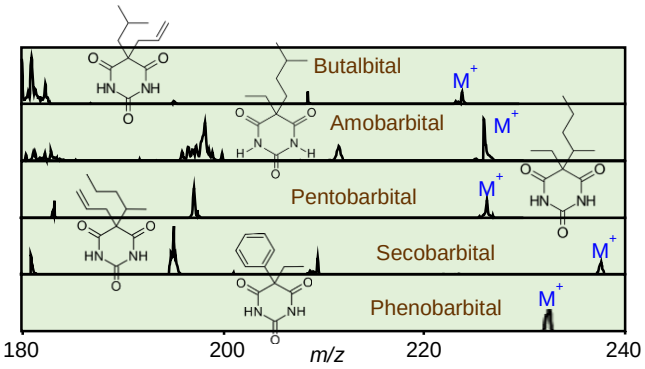

For Table of Contents Only